Cell. Mol. Life Sci. (2016) 73:2969–2984
DOI 10.1007/s00018-016-2150-0

Cellular and Molecular Life Sciences

ORIGINAL ARTICLE

The interferon α-responsive gene, Ifrg15, plays vital roles during mouse early embryonic development

Ye Yang[1] · Jiayi Wang[1] · Chun Zhao[1] · Xiaojiao Chen[1] · Li Chen[2] · Junqiang Zhang[1] · Ran Huo[3] · Chang Liu[4] · Hua Tong[1] · Xiufeng Ling[1]

Received: 22 September 2015 / Revised: 9 January 2016 / Accepted: 26 January 2016 / Published online: 24 February 2016
© Springer International Publishing 2016

Abstract The interferon alpha-responsive gene (Ifrg15) mRNA is highly expressed in various stages during preimplantation mammalian embryo development. Unfortunately, few studies have investigated the effect of Ifrg15 in this process. In mammals, the fusion of male and female pronuclei generates a diploid zygote, and is an important step for subsequent cleavage and blastocyst formation. Here, by using RNA interference, rescue experiments, immunofluorescence staining and live cell observations, we found that preimplantation embryo development was arrested at the 1-cell stage after knocking down Ifrg15 expression. This induced DNA damage and prevented the cleavage of embryos. Furthermore, the effect of Ifrg15 deficiency in arresting preimplantation embryo development produced by specific short interfering RNA microinjection was concentration-dependent. Using transcriptome expression profiles, gene ontogeny functional annotation and enrichment analysis, we gained 197 enriched pathways based on 1445 differentially expressed genes (DEGs). Of these, 12 pathways and about one third of the DEGs were involved in DNA damage, DNA repair, cell cycle, and developmental processes. Thus, the IFRG15 protein might be an important molecule for maintaining genomic integrity and stability through upregulating or downregulating a cascade of genes to permit normal preimplantation embryo development.

Keywords Preimplantation embryo development · Pronuclear fusion failure · Ifrg15 · DNA damage

Electronic supplementary material The online version of this article (doi:10.1007/s00018-016-2150-0) contains supplementary material, which is available to authorized users.

✉ Hua Tong
thua8@163.com

✉ Xiufeng Ling
lingxiufeng_njfy@163.com;
xiufengling@hotmail.com

[1] State Key Laboratory of Reproductive Medicine, Department of Reproduction, Nanjing Maternity and Child Health Care Hospital Affiliated to Nanjing Medical University, Nanjing Medical University, Nanjing 210004, Jiangsu, China

[2] Department of Reproduction, Changzhou Maternity and Child Health Care Hospital Affiliated to Nanjing Medical University, Nanjing Medical University, Changzhou 213003, Jiangsu, China

[3] State Key Laboratory of Reproductive Medicine, Department of Histology and Embryology, Nanjing Medical University, Nanjing 210004, Jiangsu, China

[4] Jiangsu Key Laboratory for Molecular and Medical Biotechnology and College of Life Sciences, Nanjing Normal University, Nanjing, Jiangsu, China

Introduction

Preimplantation embryo development is a very important process. Unraveling the underlying regulatory molecular mechanisms is of pivotal importance for developmental biology and basic reproductive biology, and might be advantageous for regenerative medicine and for the improvement of assisted reproductive technology for treating infertility [1].

For preimplantation embryo development to proceed normally, several events must take place, which span several important stages, such as fertilization, pronucleus fusion, cleavage stages (2-cell to 8-cell stage), compaction and morula formation, followed by cavitation with the formation of a blastocyst. Any abnormal steps can result in a decrease in the rate of blastocyst formation or even arrest.

For instance, fertilization initiates the completion of the meiosis II (MII) of oocytes, followed by the formation of haploid paternal and maternal pronuclei. In humans, the pronuclei are formed by the development of nuclear envelopes around the male and female chromatin and rapid decondensation. Each pronucleus then undergoes DNA replication before entering the first mitosis to produce a *2-cell embryo containing two diploid nuclear* [2]. Morphologically, the haploid male and female pronuclei move to the center of the egg where fusion occurs. It is characterized by tight association of both pronuclear envelopes with close alignment of the nucleoli [3]. Then the membranes break down. Chromosomes then orientate on the metaphase spindle for mitosis. This combination of the two genomes is called syngamy [4]. Following male and female pronuclear fusion, the formation of a diploid 1-cell zygote is crucial for the subsequent cleavage stages. The fusion of male and female pronuclei not only restores the diploid DNA content but also the centrosomes to ensure proper centrosomal number in each cell and produce equal centrosome distribution to daughter cells during cell division. This prototype of pronuclear interaction was first described by Wilson [5] in the roundworm *Ascaris*. These processes require the participation of both maternal and paternal genomes [6], and involves significant but transient changes in gene expression. Although many genes have been identified as being involved in each stage, global gene expression profiling has characterized the stages, which are regulated by complex gene regulatory networks, including many new unknown genes [7].

Ifrg15 is a recently identified interferon alpha-responsive gene that was first found by cDNA subtraction between the mandibular tissues at mouse embryo day (E)10.5 and E12, and is considered to be involved in the initiation of odontogenesis [8]. The IFRG15 protein is encoded by the Toraip2 gene (Genome Reference Consortium, GRCm38: CM000994.2: 156035403: 156068861:1 http://asia.ensembl.org/Mus_musculus/Transcript/ProteinSummary?db=core;g=ENSMUSG00000050565;r=1:156035403-156068861;t=ENSMUST00000111757), which encodes nine transcripts. No proteins are translated by transcripts 8 and 4. Transcripts 1 and 2 encode the LULL1 protein of 502 amino acids. Transcripts 5, 6, 7, and 9 encode the IFRG15 protein of 113 amino acids. Subsequently, investigators found that the IFRG15 protein is highly conserved and expressed in many mammals, including the human, monkey, rabbit, and horse, and is implicated in a wide variety of physiological roles in mammals [9]. Ifrg15 mRNA was detected in rabbit oocytes and preimplantation embryos and the expression of Ifrg15 mRNA was observed in the inner cells of the rabbit blastocysts by in situ hybridization [10]. Unfortunately, there are only a few reports on the effects of Ifrg15 on mouse embryo development, especially during preimplantation stages.

There is no doubt that there are species-specific differences in gene expression between the human and mouse genomes. However, because of the limited amounts of human-derived material and ethical concerns, researchers can only use spare human preimplantation embryos derived from in vitro fertilization to obtain insights into aspects of embryo morphology and culture conditions, using cryopreservation and thawing of human embryos in research aimed at promoting blastocyst formation. Thus, gaining insight into the cellular and molecular mechanisms of various events in human embryogenesis becomes increasingly important. Some animal models, such as the mouse embryos, are highly regulated systems, and have provided much information on preimplantation development.

Here, we present evidence that Ifrg15 plays a crucial role in early stages of mouse preimplantation embryo development, especially at the stage of the cleavage of embryos. Further research on how IFRG15 affects cell cycle during preimplantation embryo development was also performed using transcriptome sequencing and identification of candidate genes.

Materials and methods

Ethics statement

CD1 strain mice were maintained under a controlled environment of 20–25 °C, 12/12 h light/dark cycle, and 50–70 % humidity, with free access to water and food. All animal procedures were approved by Nanjing medical university, Institutional Animal Care and Use Committee, and conducted according to its Guide for the Care and Use of Laboratory Animals.

Embryo collection and culture

Female CD1 mice at 6–8 weeks of age were superovulated by injections of 10 IU hCG followed 48 h later by 10 IU of pregnant mare serum gonadotropin. MII stage oocytes were collected at 16 h post hCG from the ampullae of oviducts. Zygotes were collected at 16 h post hCG from the ampullae of oviducts of superovulated females that had been mated with the same strain of males. The cumulus cells were removed by digestion with hyaluronidase (Sigma, H3506) for several minutes. Embryos were cultured in fresh KSOM medium (Millipore, MR-020P-D) at 37 °C under 5 % CO_2 in humidified air [16]. Then, 2-cell, 4-cell, 8-cell, morula, and blastocyst stage embryos were collected after 22–26, 48–50, 60–65, 70–75, and 96–100 h of culture, respectively.

siRNA microinjection

To knock down Ifrg15 in mouse embryos, Ifrg15 siRNA 1# sense: 5′-GGACCUAUGGUUCCGUGUUTT-3′, antisense: 5′-AAAACACGGAACCATAGGTCC-3′. Ifrg15 siRNA 2# sense: 5′-UGUUACCAAGUGUUCUUAGACCGUA-3′, antisense: 5′-UACGGUCUAAGAACACUUGGUAAA-3′ (Genechem) were diluted in buffer to 100 mM. Aliquots of 5–10 pl of the siRNAs were microinjected into the cytoplasm of mouse zygotes in M2 medium (Sigma-Aldrich, M7167) and then cultured in fresh KSOM medium. Nonsilencing siRNA 5′-UUCUCCGAACGUGUCACGUTT-3′ was used as control. Zygotes cultured for 24 h (2-cell stage) were collected for detecting the knockdown efficiency by qRT-PCR.

Plasmid construction and in vitro transcription

The eukaryotic expression vector for IFRG15 was made by cloning the IFRG15 open reading frame into a pCS2 vector along with a Myc tag. The forward primer contained an FseI enzyme digestion site, and the reverse primer contained an ASCI enzyme digestion site and the sequences are shown in (Table S5). PCR was performed using cDNA as a template, and then the product was identified by gel electrophoresis and sequencing. Both the clone and the vector were digested with FseI and ASCI. Then, the open reading frame of IFRG15 was tagged with NH_2-terminal Myc6 and inserted into a pCS2 vector. The Myc6–Ifrg15–pCS2+ plasmid was linearized by SalI or KpnI digestion and purified using gel extraction kits (Promega). As SP6 message machine (Ambion) was used for producing capped mRNAs, and mRNAs were purified using RNeasy cleanup kits (Qiagen). Finally, the mRNA products were separated by gel electrophoresis. Ifrg15 mRNA microinjection was performed as described above for siRNA microinjection. The same amount of RNase-free phosphate-buffered saline (PBS) was microinjected as a negative control.

Live cell imaging system

Zygotes were harvested from female ICR mice superovulated by injections of 10 IU hCG followed 48 h later by 10 IU pregnant mare serum gonadotropin, followed by natural mating with fertile male mice. The zygotes were divided into four groups: uninjected controls, nonsilencing siRNA-injected and Ifrg15-specific siRNA injected. Then, the zygotes were transferred to 30 µl drops of culture medium covered with *sterile oil* using a Live Cell Imaging System.

Quantitative real-time PCR experiments

In brief, total RNAs were isolated with Pico Pure RNA isolation kits (Arcturus, KIT0204), according to the manufacturer's instructions. cDNAs were synthesized using Prime Script Reverse Transcription reagent kits (Takara, DRR036A) in 20 µl of reaction mixture following the manufacturer's instructions. Real-time quantitative PCR was carried out in the ABI Step One Plus Real-time PCR System (Applied Biosystems). Primers were designed online using the NCBI database (http://www.ncbi.nlm.nih.gov/) and the sequences are shown in (Table S5). The expression change (Δ) of a target gene (Tg) based on the cycle threshold (Ct) was calculated as: fold change $= 2 - (\Delta Ct\ Tg - \Delta Ct,\ control)$ [16]. The following PCR cycle settings were used: 6 min at 94 °C, (30 s at 94 °C, 30 s at 60 °C, 30 s at 72 °C) × 35 times, 10 min at 72 °C and then 4 °C thereafter. Each reaction was run in triplicate with at least three independent replicates.

EdU incorporation assay

EdU incorporation assays were performed using Cell-Light EdU Apollo488 In Vitro Imaging kits (Ribobio; http://www.ribobio.com/sitecn/productinfo_208231.html). Mouse zygotes were cultured in medium containing 50 µM EdU for 10 h prior to staining according to kit instructions. Images were captured using a Zeiss LS M710 confocal laser scanning microscope.

Immunofluorescence staining

Embryos were treated for 5 min at room temperature with 0.5 % Triton X-100 in PBS followed by 1 % BSA in PBS for 1 h without washing. They were then incubated with the primary antibodies (Table S5) overnight at 4 °C. Next day the sections were washed and incubated with secondary antibodies for 3 h at room temperature in the dark. After incubation for 5 min at room temperature with Hoechst 33342 (Molecular Probes, H21492), the embryos were washed and then cover slipped with DABCO and examined using a Zeiss LS M710 confocal laser scanning microscope.

Transcriptome sequencing and analysis

The transcriptome sequence and analysis was performed by ANNOROAD Gene Technology company. Zygotes were harvested from female ICR mice superovulated by injections of 10 IU hCG followed 48 h later by 10 IU pregnant

mare serum gonadotropin, followed by natural mating with fertile male mice. The zygotes were divided into three groups: uninjected controls, nonsilencing siRNA-injected and Ifrg15-specific siRNA injected. Then, the 100 zygotes of each group were cultured and collected at 36 h post hCG and transferred to 10 μl buffer (provide by ANNOROAD Gene Technology company) and stored at −80 °C.

1. The amplification of single cell transcriptome and cDNA products detection. (1) The samples collected by single cell collection tube were amplified directly with the Smart-Seq 2 method: Add reverse transcription enzyme, buffer, oligo-dT primers with common sequence and TSO primers to synthesize the first cDNA strand. The second cDNA strand was synthesized by adding PCR amplification reagent and ISPCR primer with common sequence to the first cDNA strand products. The aimed products were purified and recovered with Beckman Ampure XP magnetic beads and dissolved in EB buffer. (2) RNA concentration of library was measured using Qubit2.0 Fluro meter (Life Technologies, CA, USA). (3) Agilent 2100 High Sensitivity DNA Assay Kit (Agilent Technologies, CA, USA) was used to detect the fragments distribution of the amplified products. (4) According to the results, the quality of the amplified products was evaluated.
2. Library construction for single cell transcriptome. (1) A total amount of 20 ng amplified products cDNA per sample was used as input material for the Library construction of single cell transcriptome. (2) Fragmentation was carried out with Bioruptor® Sonication System (Diagenode Inc.) for cDNA to 200 bp in length. (3) The reaction of terminal repair, the addition of A, and ligation of sequencing adapters were performed on the above fragments products with magnetic purification of Beckman Ampure XP for each reaction. The products with sequencing adapters were amplified by PCR, and the samples were added with different Index tags to distinguish each samples during the sequencing process. (4) The PCR amplification products were screened by 2 % agarose gels to get 300–350 bp DNA fragments in length. Recover DNA from the agarose gels with CWBIO Gel Extraction Kit and dissolve the min EB buffer to get the final Library.
3. Library examination. After the library construction, insert size was assessed using the Agilent Bio analyzer 2100 system (Agilent Technologies, CA, USA), and the qualified insert size was accurate quantificated using Taqman fluorescence probe of AB Step One. Plus Real-Time PCR system (Library valid concentration >2 nM).
4. Library clustering and sequencing. The clustering of the index-coded samples was performed on a cBot cluster generation system using TruSeq PE Cluster Kit v2-cBot-HS (Illumina) according to the manufacturer's instructions. Then the libraries were sequenced on an Illumina Hiseq 2500 platform and100 bp paired-end reads were generated.
5. Data quality control. In order to guarantee the data quality for analysis, the Perl script was used to filter the original data (Raw Data). The filtering process of the Perl script: (1) Remove the adapter polluted reads The adapter polluted reads was defined as: the read bases contained more than 5 bp of the adapter sequences. If either one of the PE Reads was polluted, pair ends of the reads would be removed; (2) Remove the low quality reads The low quality reads was defined as the number of reads with phred quality value less than or equal to 19 accounted for more than 15 %. If either one of the PE Reads defined as low quality, pair ends of the reads would be removed; Remove the reads with N base contamination more than 5 % of total bases. If either one of the PE Reads has high Ns bases, pair ends of the reads would be removed. After the filtering process, the clean data was assessed data quantity including Q30 statistics, data quantity statistics, base content statistics, etc.
6. The sequence mapping. Reference gene and genome annotation files downloaded from the UCSC (http://hgdownload.soe.ucsc.edu/goldenPath/galGal4) was used for building the reference genome library with Bowtie2 v2.2.3. Then the clean data was mapped to the reference genome by software TopHat v2.0.12. The Tophat is specialized for transcriptome data analysis. To achieve the purpose of identification exon–exon splicesites, the reads were splitted to map references. At the same time, the Bowtie2 was also used for mapping and compared data with TopHat to make the mapping result more accurate.
7. The expression quantity estimation. HTSeqv0.6.0 was run to calculate the counts of each gene, and RPKM was used to assess the expression quantity. RPKM (Reads Per Kilobase of exon model per Million mapped reads) values considering the effect of sequencing depth and gene length for the reads count at the same time, was used to calculate gene expression levels.
8. Differential expression analysis. DESeq package was used for differentially expressed analysis of genes. The significance of the differentially genes were calculated with the DESeq software, doing a pair-wise comparison between all the biological replicates of the enriched/enhanced tissue (or group of tissues) and all the other tissues. The multiple-testing adjusted p value (FDR 5 %) was used to determine whether the gene is significantly differential expressed or not.

9. Bioinformatics analysis. Gene ontology (GO; Biological Process and Cellular Component) analysis was performed using the online tools http://amigo.geneontology.org/amigo and http://www.genome.jp/feedback/. Pathway analysis was performed using the KEGG PATHWAY database (http://www.kegg.jp).

Statistics

Each experiment was repeated at least three times. In the results of Quantitative real-time PCR Experiments, all data are presented as the mean and standard error of the mean (mean ± SEM). ANOVA with post hoc testing were performed to test the differences between normal, negative control and IFRG15 siRNA injected groups, $p < 0.05$ was considered significant. In the experiments of embryo development, numbers of embryos examined are indicated (n). Chi square test was used in these studies. $p < 0.05$ was considered statistically significant.

Results

IFRG15 plays crucial roles during mouse preimplantation embryo development

Unfortunately, because there is no commercially available IFRG15 protein-specific antibody (Supplementary Figure 1A), we could not determine the quantity and the location of IFRG15 protein expression by western blotting or immunohistochemistry. However we found that the Ifrg15 gene was mainly expressed in reproductive tissues such as the testis, ovary and granulosa cells by quantitative real-time polymerase chain reaction (qRT-PCR) analysis (Fig. 1a).

We also detected the relative expression level of Ifrg15 at various phases of embryo development such as the germinal vesicle, MII, zygote, 2-cell, 4-cell, 8-cell, morula, and blastocyst stages. As shown in Fig. 1b, the expression level of Ifrg15 was the lowest in the MII and zygote stages, and peaked at 2-cell stage. Thereafter, the expression levels declined gradually, and then showed a slight increase.

IFRG15 is encoded by the Toraip2 gene that can generate two different transcripts (Supplementary Figure 2A). Therefore, we were interested in the expression of the other transcript, LULL1 protein, and wondered whether it had a similar function to IFRG15. Comparing and analyzing the relative expression levels of Lull1 mRNA at various phases of development such as the germinal vesicle, MII, zygote, 2-cell, 4-cell, 8-cell, morula and blastocyst stages (Supplementary Figure 2B), we found that the expression levels of Lull1 peaked at the 2-cell stage and then reduced gradually with further development. We also interfered with Lulll1 mRNA expression using a specific siRNA fragment (Supplementary Figure 2C). The results showed that no any difference of development of embryo was observed between experiment group and negative control group (Supplementary Figure 2D). Moreover, comparing the amino acid sequences between IFRG15 and LULL1 showed almost no homology between them. Thus, unlike IFRG15, LULL1 had no discernable effect on mouse preimplantation embryo development.

To determine the effects of Ifrg15 on mouse preimplantation embryo development, we first knocked down its expression level by microinjecting short interfering (si)RNA duplex oligo ribonucleotides specific for the gene coding region of Ifrg15: siRNAs #1 and #2 (GenBank: AJ251363.1) into fertilized mouse zygotes. Two Ifrg15-specific siRNAs, whose knockdown efficiencies were verified by real-time PCR (Fig. 2a), were microinjected into mouse zygotes.

We next monitored the development of these zygotes. As shown in Fig. 2b, c, the normal and the non-silence siRNA injected zygotes developed normally to the 2-cell stage. There was no significant difference between the two groups with 2-cell formation rates of 97 and 98 %, respectively. However, 28 and 40 % of zygotes injected with siRNAs #1 or #2, respectively, stopped at the 1-cell stage. We continued to monitor the development of those zygotes and calculated the percentages of each stage. The blastocyst formation rate of in those zygotes injected with siRNAs #1 or #2 were significantly lower than negative control groups (negative control groups, 87 %; siRNAs #1, 15 %, $p < 0.001$; siRNAs #2, 13 %, $p < 0.001$). These results imply that the IFGR15 protein probably plays critical biological roles during early embryo development. We continue to culture the zygotes which arrest at 1-cell stage, they did not continue development and died gradually (Fig. 3a). Next, we aimed to determine whether the effect of knocking down Ifrg15 on the first cleavage of mouse zygotes was specific. Those zygotes that had developed to the 2-cell stage were selected randomly, and one of blastomeres was microinjected with siRNAs against Ifrg15 or a non-silence siRNA. As shown in Fig. 3b, only those zygotes in which one of blastomere was injected with Ifrg15-specific siRNA developed to the 3-cell stage, while zygotes of normal and negative control groups developed normally to the 4-cell stage. Thus, the effect of IFRG15 deficiency on cell division during embryos development did not occur specifically at the first zygotic cleavage.

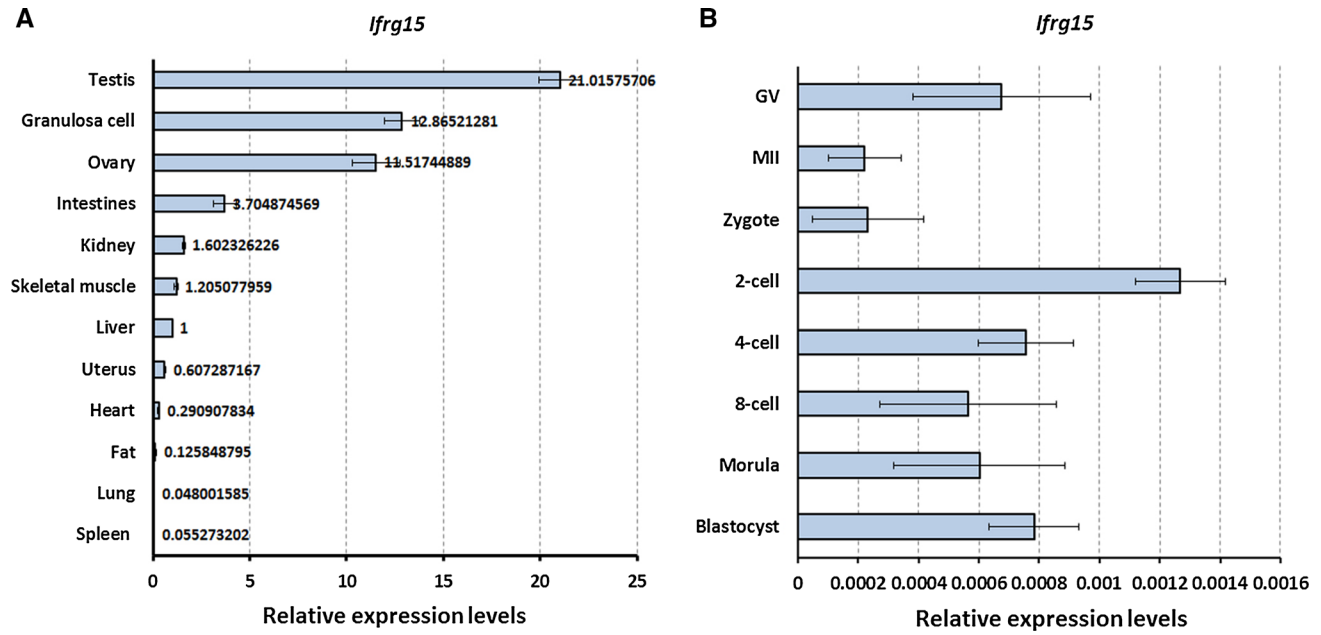

Fig. 1 The expression of Ifrg15 in different tissues and at various time points during early embryonic development. **a** Relative analysis of Ifrg15 mRNA by qRT-PCR. Ifrg15 mRNA is ubiquitously expressed in various tissues and organs. Testis, ovary and granulosa cells had the highest expression levels. **b** Ifrg15 mRNA was expressed in the germinal vesicle phase oocyte (GV), metaphase II phase oocyte (M II), zygote, 2-cell, 4-cell, 8-cell, morula and blastocyst stages. The lowest expression was seen in the MII and zygote stages, and reached a peak at the 2-cell stage. The expression level reduced gradually, and then showed a slight increase. Three batches of embryos were analyzed statistically. The *y-axis* represents the relative quantification of target genes normalized to 18sRNA as calculated by $2^{-\Delta\Delta Ct}$ method in the real-time PCR assays. $*p < 0.05$; $**p < 0.01$

siRNAs against Ifrg15 inhibited the first cleavage of mouse zygotes in a concentration-dependent manner

To clarify whether the effects of Ifrg15-specific siRNAs on preimplantation embryo development were concentration-dependent, cytoplasmic microinjection of the siRNAs was done using various concentrations including 20, 50, and 100 μM; 100 μM of a non-silence siRNA fragment was used as a negative control. As shown in Supplementary Figure 3, almost all zygotes in normal and negative control groups could develop to the 2-cell stage (99, 100 %), and the blastocyst formation rate was approximately 80 %. By contrast, only 97, 90 and 47 % of the zygotes microinjected with 20, 50, and 100 μM of the siRNA1# could develop to the 2-cell stage and the blastocyst formation rate decreased to 42, 33, and 4 %, respectively. The results of microinjection of siRNA2# were similar to siRNA1#. This demonstrated a concentration-dependent response.

Silencing Ifrg15 expression blocked the initiation of zygotic genome activation

Zygotic genome activation (ZGA) is a major event during embryonic cleavage, and occurs during the late 1-cell/early 2-cell stages. With in vitro manipulation of mammalian embryos, abnormal ZGA initiation can result in developmental arrest. To clarify whether silencing Ifrg15 expression could block ZGA, we tested the ability of Ifrg15-deficient embryos to activate the zygotic genome. We measured the expression levels of several genes that are markers of ZGA, including those encoding murine endogenous retrovirus-like (MuERV-L), heat shock protein 70.1 (HSP70.1), eukaryotic translation initiation factor A (EIF-1a) and U2afbp-rs because these genes start to be expressed at ZGA [11, 12], using qRT-PCR. The zygotes in different groups were harvested at the late 1-cell stage (36 h post HCG). Using negative control zygotes as controls, there were no statistically significant differences in the expression levels of these genes between normal and negative control groups. At same time, the zygotes treated with 1# and 2# siRNAs against Ifrg15 displayed sharply reduced expression levels of all these genes, suggesting a defect in ZGA (Fig. 3c). These results demonstrate that ZGA is severely disturbed or blocked in IFRG15-deficient embryos.

Developmental arrest caused by blocking Ifrg15 expression could be rescued by microinjecting Ifrg15 mRNA

To verify the effect of siRNA Ifrg15-specific on 1-cell arrest, rescue experiments were performed by ectopic

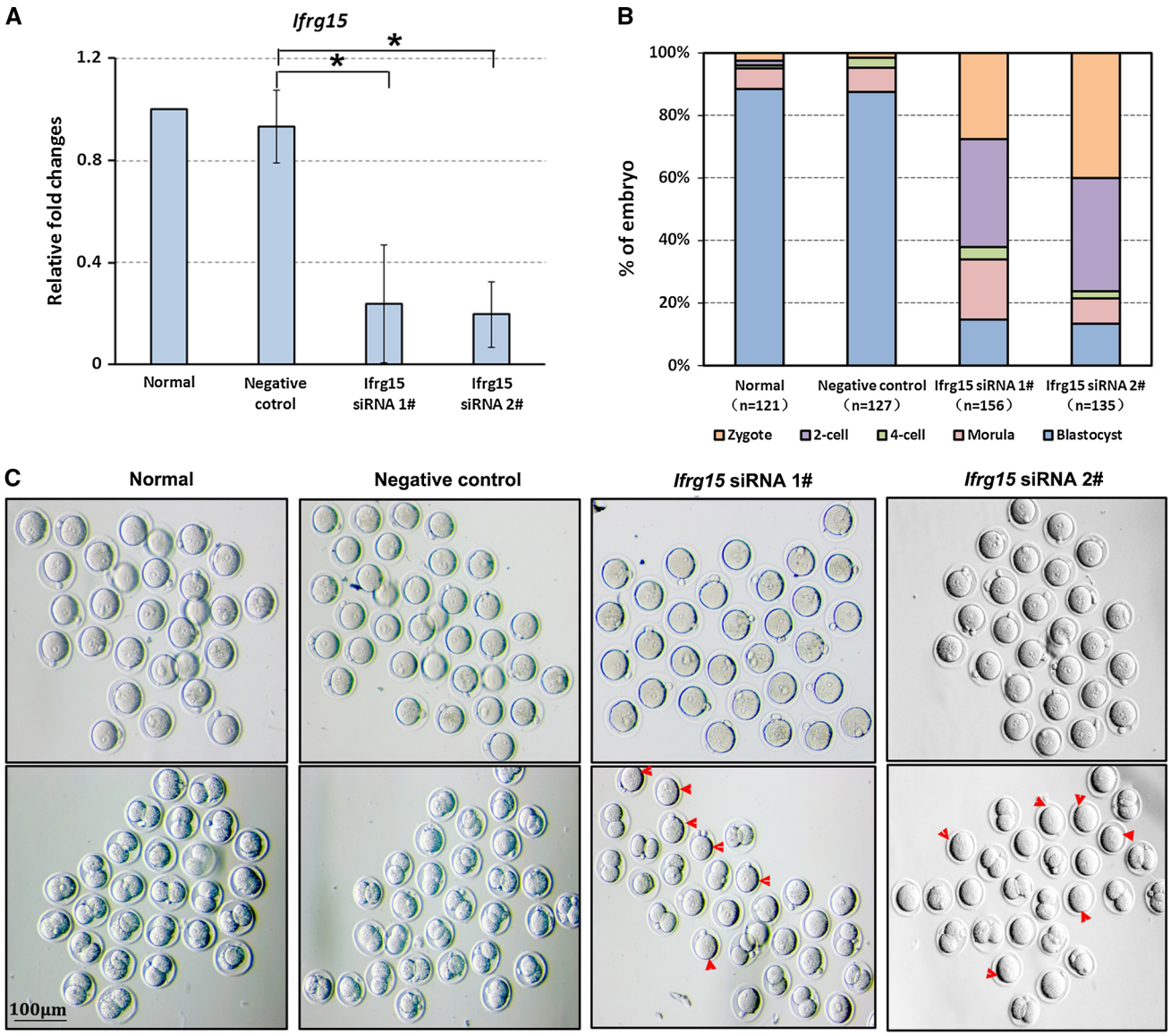

Fig. 2 Effect of Ifrg15 knockdown on early embryonic development. **a** Verifying the efficiency of Ifrg15 knockdown by qRT-PCR. The samples were collected from zygotes cultured in KSOM medium for 6 h after siRNA microinjection. Data are presented as mean values ± SD. **b** Comparison of zygotes arrest rate (the *orange bar*) and embryo formation rate (the *blue bar*) between the normal, negative control and Ifrg15 knockdown groups. The percentages of embryos that arrested at the zygote stage were evidently higher than negative control group (siRNA #1, 28 %, $n = 156$, $p < 0.001$; siRNA #2, 40 %, $n = 135$, $p < 0.001$; vs negative control). **c** Comparison of embryonic development among different groups. While the uninjected zygotes and those injected with non-silencing siRNA entered the 2-cell stage, part of those zygotes injected with Ifrg15-specific siRNAs were arrested at the 1-cell stage (*arrowheads*)

overexpression of IFRG15. An Ifrg15 gene overexpression construct containing a Myc tag was generated and the sequence was confirmed. Microinjection of Ifrg15 mRNA was performed after in vitro transcription. To confirm that the injected mRNA sequence could translate, immunofluorescence staining was performed using an anti-Myc antibody. As shown in Supplementary Figure 4, strong positive Myc signals were distributed uniformly in the cytoplasm of zygotes, suggesting that the mRNA was expressed successfully. We next performed a combined cytoplasmic microinjection of siRNAs Ifrg15-specific siRNAs together with Ifrg15 mRNA, and siRNA against Ifrg15 together with double-distilled H_2O was used as a control. The zygotes in control groups maintained a higher rate of arrest at the first cleavage stage when compared with the uninjected zygotes (normal group) (shown in Fig. 4a). However, those zygotes microinjected with a combination of siRNAs Ifrg15-specific siRNAs and Ifrg15 mRNA showed an obvious decrease in the arrest rate at 1-cell stage, and most zygotes

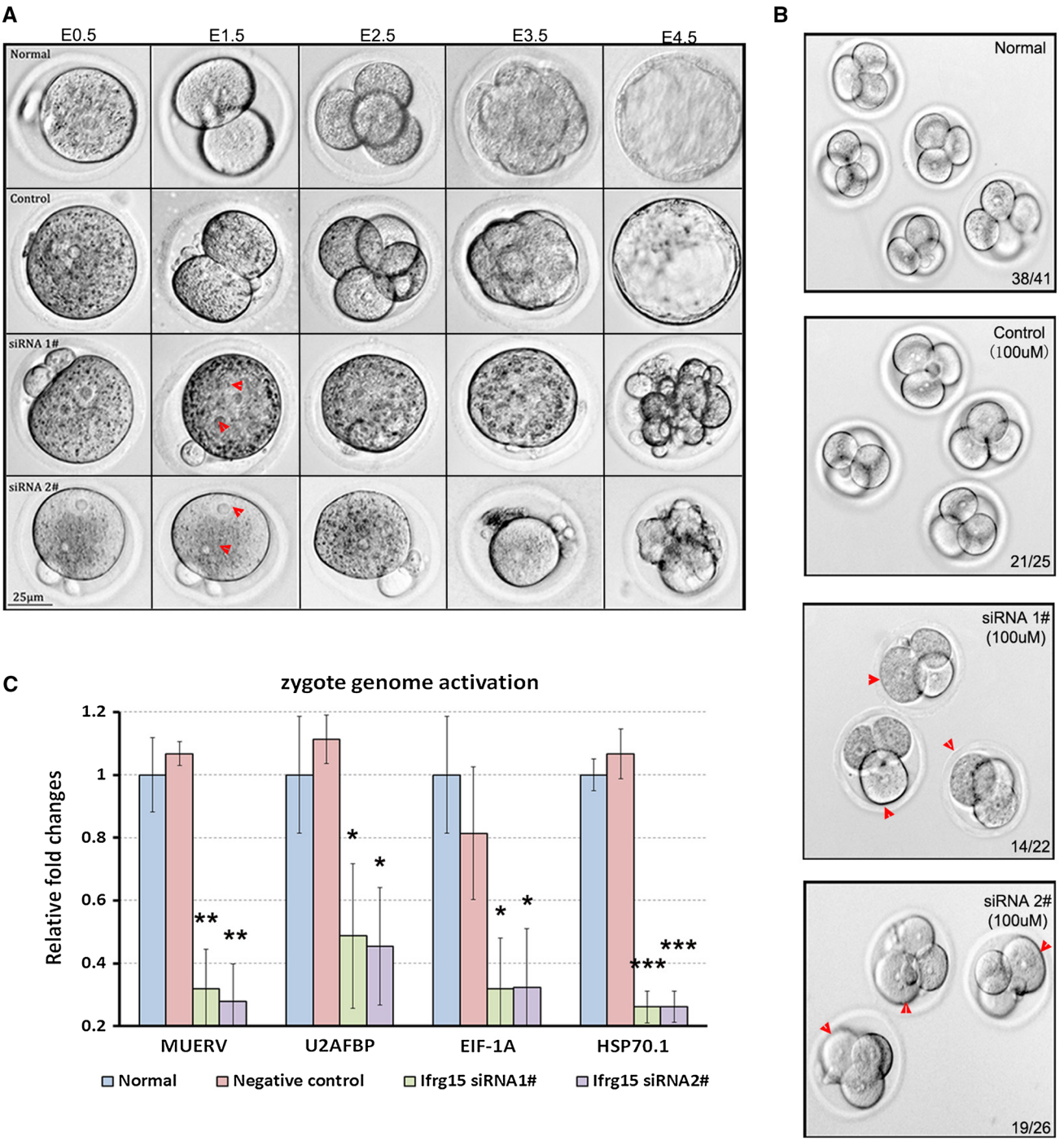

Fig. 3 SiRNA against Ifrg15 inhibited the blastomere cleavage of mouse embryos **a** Ifrg15-knockdown zygotes that did not enter the 2-cell stage were cultured but did not continue development and died gradually. **b** One of blastomere of 2-cell stage embryos was selected randomly for microinjection with siRNA fragments including those specific against Ifrg15 and non-silence siRNA. most of 2-cells in the normal and negative control groups could develop normally to the 4-cell stage (normal, 38/41; negative control, 21/25), but partly 2-cells injected with siRNAs specific against Ifrg15 developed to the 3-cell stage (siRNA #1, 14/22, $p < 0.001$; siRNA #2, 19/26, $p < 0.001$; vs negative control). **c** Blockade of Ifrg15 by siRNA microinjection led to a significant reduction in the levels of four mRNAs which are markers of ZGA (including MuERV-L, HSP70.1, EIF-1a, and U2afbp-rs). There were no statistically significant differences between the normal and negative control groups, whereas all of those genes in the zygotes injected with siRNA against Ifrg15 displayed sharply reduced expression levels. The *y-axis* represents the relative quantification of target genes normalized to 18sRNA as calculated by $2^{-\Delta\Delta Ct}$ method in the real-time PCR assays. *$p < 0.05$; **$p < 0.01$

developed to the 2-cell stage (Fig. 4b). As shown in Fig. 4c, the rates of 1-cell arrest for groups treated with siRNAs #1 and #2 combined with double-distilled H_2O were 42 and 45 %, and the blastocyst formation rates were 21 and 22 %, respectively; significantly higher than in the uninjected zygotes (normal group). In contrast, the rates of 1-cell arrest in groups microinjected with both siRNAs combined with Ifrg15 mRNA were reduced significantly (siRNA1#, 14 %, $p < 0.05$; siRNA2#, 13 %, $p < 0.05$), which led to a significant increase in the blastocyst formation rate (siRNA1#, 61 %, $p < 0.05$; siRNA2#, 62 %, $p < 0.05$). Thus, the developmental arrest derived from blocking Ifrg15 expression can be rescued by simultaneously microinjecting Ifrg15 mRNA, suggesting that the IFRG15 protein plays a vital role during mouse embryo development.

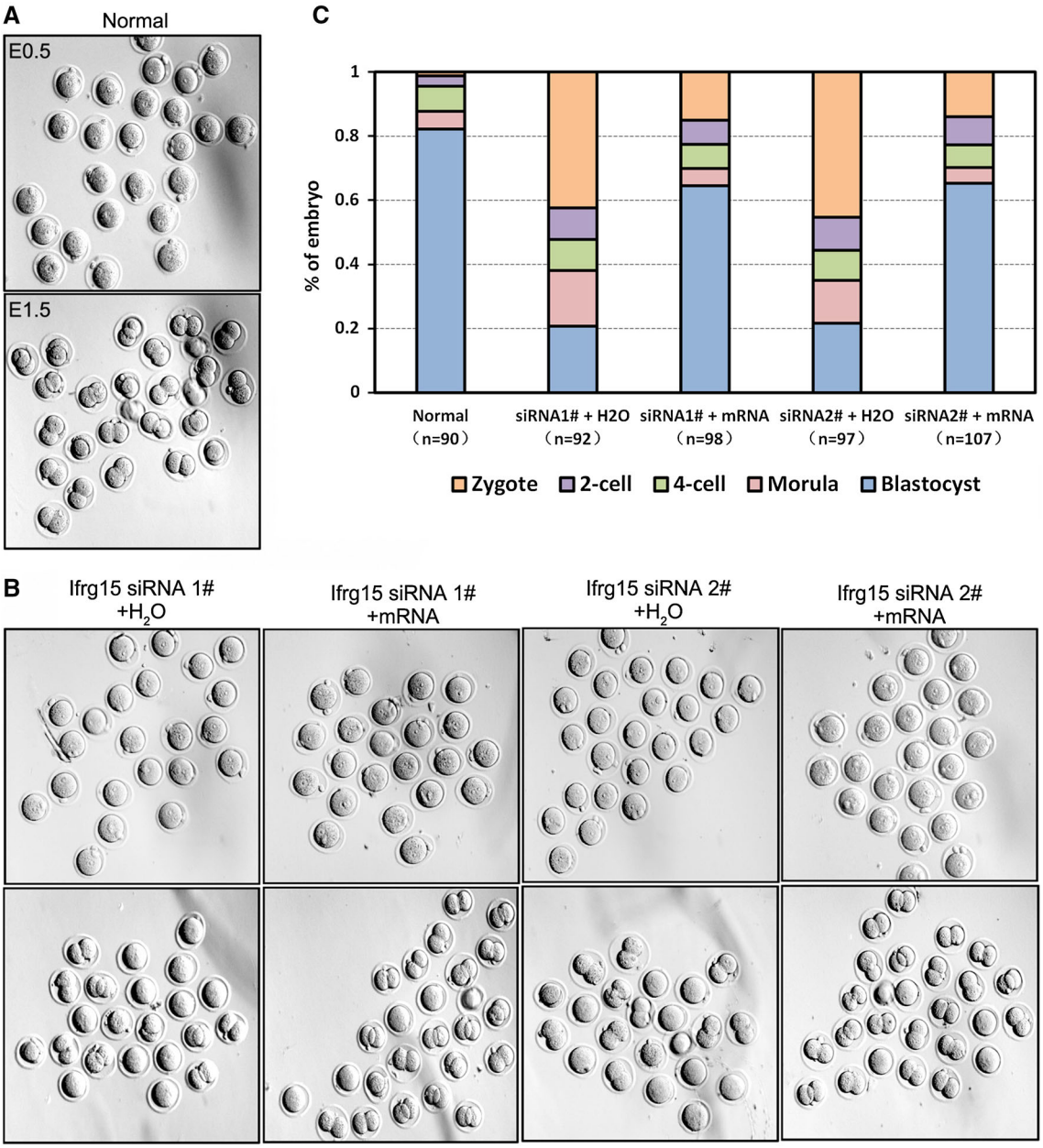

Fig. 4 Developmental arrest produced by knocking down Ifrg15 could be rescued by microinjecting Ifrg15 mRNA. The normal group was shown in (**a**). **b** The zygotes were divided into four group respectively microinjected with Ifrg15 siRNA 1# + sterile ddH_2O, Ifrg15 siRNA 1# + Ifrg15 mRNA, Ifrg15 siRNA 2# + sterile ddH_2O, Ifrg15 siRNA 2# + Ifrg15 mRNA. **c** The uninjected zygotes developed normally to the 2-cell stage (99 %). Those zygotes injected with Ifrg15 siRNA + sterile ddH_2O showed developmental defects with 42 % ($p < 0.05$) and 45 % ($p < 0.01$) of embryos arrested at the 1-cell stage respectively, versus normal group. Only 14 % ($p < 0.05$) and 13 % ($p < 0.05$) of zygotes injected with mRNA + Ifrg15 siRNA arrested at the 1-cell stage

Knocking down Ifrg15 and inhibiting the first cleavage of mouse zygotes might arise from the failure of male and female pronuclear fusion

To clarify the molecular mechanisms by which Ifrg15 affects 1-cell arrest, the development of normal zygotes and those zygotes microinjected with siRNAs against Ifrg15 or scrambled siRNA fragments were monitored at 24–43 h after human chorionic gonadotropin (hCG) administration to induce ovulation. The female and male pronuclei could be observed at 24 h post hCG, and began to migrate toward each other. Fusion finished at about 39 h post hCG in normal and control groups. After zygote formation, the cell divided and entered the 2-cell stage at about 43 h post hCG. Importantly, although the male and female pronuclei began to migrate toward each other, the two remained separate during zygote formation and fusion did not occur in groups treated with either siRNA #1 or #2 treated groups (Fig. 5a). Thus, the failure of male and female pronuclear fusion after inhibiting Ifrg15 expression led to 1-cell arrest.

DNA damage might explain the failure of male and female pronuclear fusion caused by knocking down Ifrg15 expression

To further explain these phenomena, we used 5-ethynyl-2′-deoxyuridine (EdU) DNA incorporation to determine whether those zygotes injected with siRNAs specific against Ifrg15 could enter the DNA synthesis (S) phase of the cell cycle, and whether DNA could replicate. This was because is widely accepted that fusion of the male and female pronuclei occur in the mitotic (M) phase following a very short gap 2 (G2) phase of 1 h. EdU incorporation experiment was performed among normal, negative control and Ifrg15 siRNA microinjection groups. Due to different developmental phase of embryo, at the early zygote stage, 79.3 and 82.9 % had not yet shown pronuclear fusion. Chromosomal condensation had occurred in 64 and 63.8 % of the zygotes and they had entered the M phase at late zygote stage in all the normal and negative control groups zygotes. However 91 and 92.8 % of arrested zygotes stopped development before pronuclear fusion in the groups injected with Ifrg15-specific siRNAs at the very late zygote stage. In addition, more EdU could be incorporated into the male and female pronuclei in groups treated with two Ifrg15-specific siRNA fragments compared with normal and negative control groups.

As EdU incorporation can be attributed to DNA replication or DNA damage, to answer this question, immunofluorescence staining was performed with antibodies against phosphorylated H2AX histone (γH2AX) and ataxia telangiectasia mutated (ATM). Experimental and control zygotes were collected at the same time points. Very weak γH2AX positive signals were observed in both normal and control groups. We believe that these signals implied that chromosomes with normal structure had entered the M phase. As expected, very strong γH2AX positive signals were noted in the zygotes injected with siRNAs, which failed to undergo pronuclear fusion (Fig. 5c). Similarly, no ATM positive signals were observed in normal and control zygotes, and there were very strong positive ATM signals in chromatin regions in siRNA-treated zygotes (Fig. 5d). Thus, DNA damage might be one reason for the failure of male and female pronuclear fusion caused by knocking down Ifrg15.

Fig. 5 Microinjection with siRNA specific against Ifrg15 inhibited the cleavage of mouse zygotes, possibly because of DNA damage. **a** Zygotes were divided into four groups. Normal zygotes and those microinjected with siRNA specific against Ifrg15 or with a scrambled siRNA fragment were monitored in the Live Cell Station at 24–43 h post hCG injection to induce ovulation. Male and female pronuclear fusion occurred and was complete at 39 h post-hCG injection in normal and control groups. The zygotes divided and entered the 2-cell stage at about 43 h post hCG. The male and female pronuclei begin to migrate toward each other, but fusion did not occur in groups treated with siRNA #1 or #2. **b** Immunofluorescence staining for EdU incorporation combined with confocal microscopy analysis demonstrated that EdU positive signals are noted in normal and control groups, the zygotes injected with siRNAs specific against Ifrg15 show a little strong EdU positive signals. At the early zygote stage, 79.3 and 82.9 % had not yet shown pronuclear fusion. Chromosomal condensation had occurred in 64 and 63.8 % of the zygotes and they had entered the M phase at late zygote stage in all the normal and negative control groups zygotes. However 91 and 92.8 % of arrested zygotes stopped development before pronuclear fusion in the groups injected with Ifrg15-specific siRNAs at the very late zygote stage. **c** Experimental and control zygotes were collected at the same time points. Very weak γH2AX positive signals were observed in those that had entered the M phase in the normal and control groups. Very strong γH2AX positive signals were noted in those fertilized eggs injected with siRNAs specific against Ifrg15. **d** No ATM-immuno positive signals were observed in the normal and control groups, but positive signals were present in the chromatin region of those treated with siRNAs specific against Ifrg15

Comparison of transcriptomes between normal, control and Ifrg15-specific siRNA-treated group

Transcriptome analysis can provide information about gene expression profiles and functions, and been widely applied to investigate gene expression at the RNA level. However, little is known about the gene expression profile of zygotes treated with siRNA for Ifrg15. Illumina Hiseq 2500 platform (http://www.illumina.com/systems/hiseq_2500_1500.html) was used for transcriptome sequencing. Transcriptomes were compared, and differentially expressed genes (DEGs) were analyzed in three samples for each group: normal, and microinjected with non-silence siRNA or

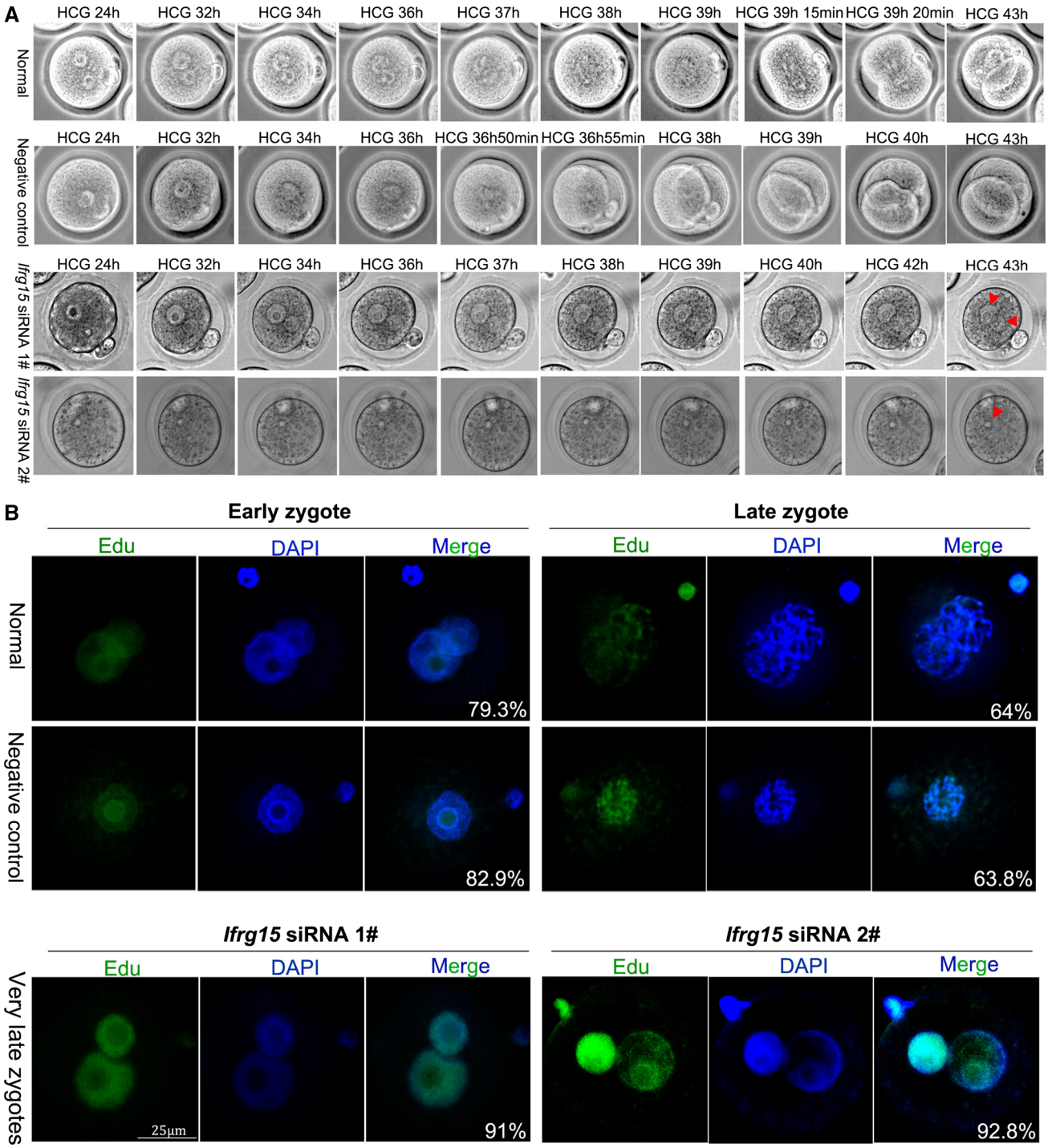

Ifrg15-specific siRNA. After quantitative assessment, to determine the DEGs we filtered the reads with a false discovery rate ≤0.05 and a |log2 (ratio)| ≥ 2. No DEGs were found between negative control group and normal group, and 1445 DEGs were generated between Ifrg15-specific siRNA-treated and the negative control group. Of these DEGs, 1086 were upregulated and 359 were down-regulated (Fig. 6a; Table S1).

In Fig. 6b and Table S2, we have categorized the DEGs identified in this study in terms of molecular function and biological processes based on GO analysis. The majority of DEGs (907; 63 %) were mainly involved in the molecular function of 'binding', followed by genes of involved in 'catalytic function' (470; 33 %), 'molecular function regulator' (101; 0.07 %) and others. In 23 GO biological process categories, the dominant pathways

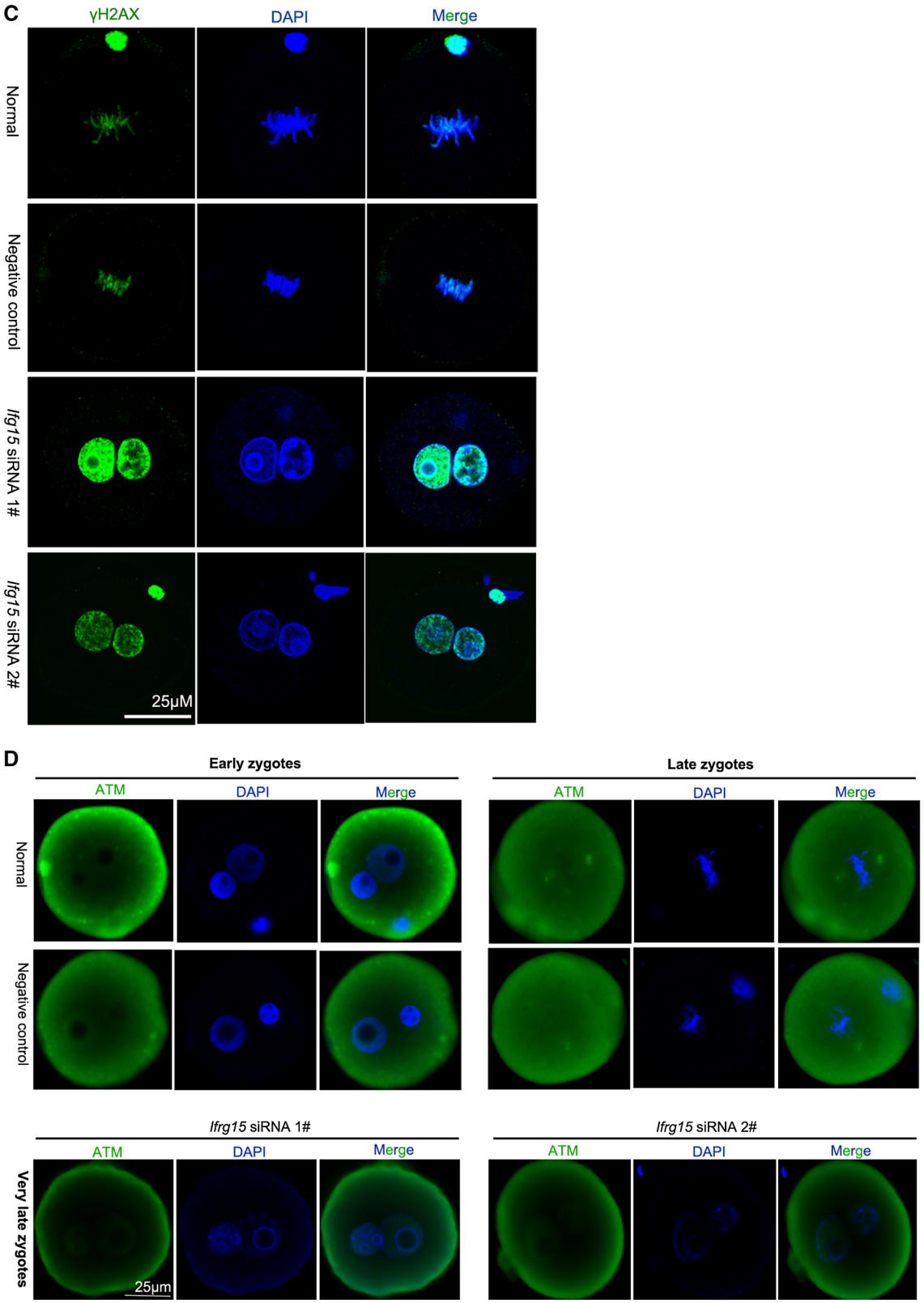

Fig. 5 continued

were the following: 'metabolic process', 'cellular process', 'response to stimulus', 'biological regulation' 'development process', and 'reproductive process', in which 758 upregulated DEGs and 189 downregulated DEGs were mainly involved in the annotation 'cellular process'.

GO and pathway analysis of the identified DEGs

We performed GO enrichment analysis on the 1445 DEGs to analyze biological function and molecular pathways between Ifrg15-specific siRNA-treated and control groups. Of 197 enriched biological process pathways (Table S3), 12 were closely associated with DNA damage. These were 'cell cycle', 'cell cycle process', 'developmental process', 'DNA integrity checkpoint', 'DNA repair', 'embryo development', 'regulation of cell cycle', 'regulation of developmental process', 'regulation of DNA damage checkpoint', 'regulation of response to DNA damage stimulus', 'response to DNA damage stimulus' and 'negative regulation of developmental process'. Combined with our detection results for EdU and DNA damage, we therefore believe that an IFRG15 deficiency can lead to DNA damage. To verify the results of transcriptomic expression profiles, 55 representative genes were selected from upregulated and downregulated DEGs for subsequent qRT-PCR experiments (Fig. 7; Supplementary Figure 4; primer information is shown in Table S1). The qRT-PCR results showed that the expression trends of these genes were consistent with the transcriptomic expression profiles. In summary, these results reveal that the DEG analysis in this study was credible, and the alteration of some processes and pathways, such as 'DNA damage', 'response to DNA damage stimulus', and 'DNA integrity checkpoint', suggest how knocking down Ifrg15 expression interrupted key molecular mechanisms and caused cleavage arrest in zygotes.

The Kyoto Encyclopedia of Genes and Genomes (KEGG) PATHWAY database (http://www.kegg.jp) was also used for pathway analysis on the 1445 dDEGs. As shown in Fig. 6c and Table S4, the results implicated major critical signaling pathways, such as those involved in ribosomal function, the Hippo signaling pathway and cell cycle, ubiquitin-mediated proteolysis, and regulation of the actin cytoskeleton.

Discussion

Understanding the molecular mechanisms involved in preimplantation embryonic development is important both for basic reproductive biology and for practical applications. The data from this study suggest that Ifrg15 and its downstream target genes play vital roles in maintaining DNA integrity and protecting the genome from damage. With Ifrg15 deficiency, DNA integrity was disrupted and DNA was damaged so that the cleavage failed and preimplantation embryo development was blocked at the 1-cell stage.

In this project, we found that Ifrg15 was differentially expressed in each of the embryonic stages studied, and expression peaked at the 2-cell stage. This suggested that the IFRG15 protein might play crucial roles in preimplantation embryonic development. Therefore, we further studied the effect of IFRG15 on mouse preimplantation embryos using siRNA, ectopic overexpression, immunofluorescence staining, live cell studies as well as transcriptome expression profiling. We found that the blastocyst formation rate decreased significantly after knocking down Ifrg15, and most embryos were arrested at the zygote and 2-cell stages. Using live cell monitoring, 1-cell arrest was observed following the failure of fusion of male and female pronuclei. In addition, we also found that the effect of IFRG15 deficiency on 1-cell arrest was highly dependent on the concentrations of siRNAs administered. Importantly, this phenomenon could be rescued by microinjecting Ifrg15 mRNA. Then, we found those 2-cells in which one of the cells was injected with a siRNA Ifrg15-specific developed to the 3-cell stage but not 4-cells. Hence the effect of IFRG15 deficiency on cell division during preimplantation development did not occur specifically at the first zygotic cleavage.

Subsequently, we found that the expression of *lull1* was different with *Ifrg15* in each of the embryonic stages. The expression levels of Lull1 peaked at the 2-cell stage and then reduced gradually with further development. We further studied the effect of LULL1 on mouse preimplantation embryos using siRNA, the results showed that no any effect on embryos development. The mechanism of Ifrg15 affecting the developmentment of embryos was independent with lull1.

We further analyzed why IFRG15 deficiency led to the failure of cleavage of embryos. Normally, within 24 h of fertilization, male and female pronuclei replicate their DNA in the 1-cell zygote and then their chromosomes undergo congression at syngamy prior to mitosis, cytokinesis and formation of the 2-cell embryo [13]. We therefore tested whether DNA could replicate in male and female pronuclei by EdU incorporation after knocking down Ifrg15. Unexpectedly, we found that more EdU could be incorporated into the male and female pronuclei in groups treated with two Ifrg15-specific siRNA fragments when compared with normal and negative control groups. Given that EdU is incorporated during DNA replication, the repair of DNA damage also requires nucleotide incorporation we performed DNA damage detection. DNA

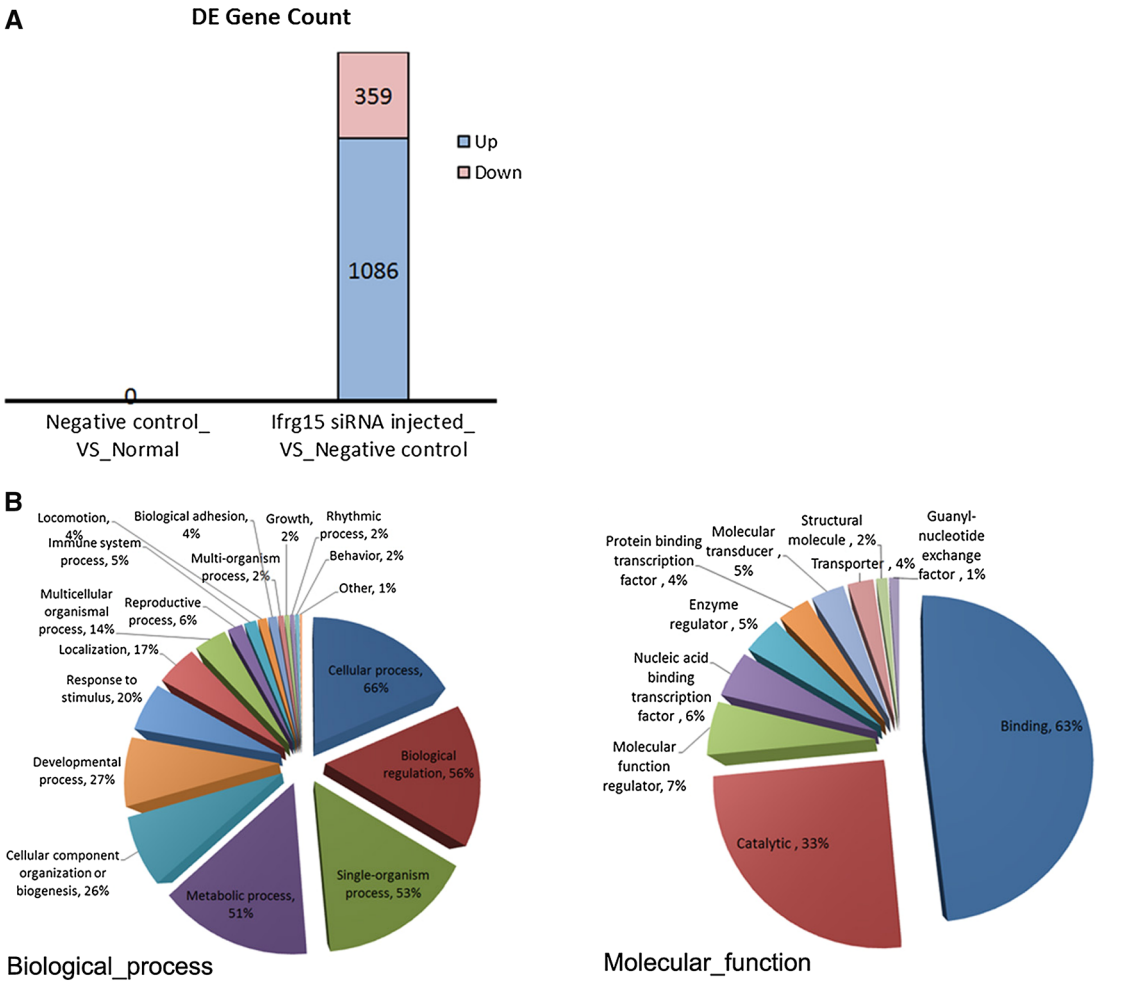
A
DE Gene Count
359
1086
0
Up
Down
Negative control_ VS_Normal
Ifrg15 siRNA injected_ VS_Negative control
B
Locomotion, 4%
Biological adhesion, 4%
Growth, 2%
Rhythmic process, 2%
Immune system process, 5%
Multi-organism process, 2%
Behavior, 2%
Other, 1%
Multicellular organismal process, 14%
Reproductive process, 6%
Localization, 17%
Response to stimulus, 20%
Cellular process, 66%
Biological regulation, 56%
Developmental process, 27%
Cellular component organization or biogenesis, 26%
Metabolic process, 51%
Single-organism process, 53%
Biological_process
Protein binding transcription factor, 4%
Molecular transducer, 5%
Structural molecule, 2%
Transporter, 4%
Guanyl-nucleotide exchange factor, 1%
Enzyme regulator, 5%
Nucleic acid binding transcription factor, 6%
Molecular function regulator, 7%
Binding, 63%
Catalytic, 33%
Molecular_function
C
KEGG pathway analysis
-LOG10(P)
20
16
12
8
4
0
Ribosome
Olfactory transduction
Hippo signaling pathway - fly
Ubiquitin mediated proteolysis
Tight junction
Regulation of actin cytoskeleton
Protein processing in endoplasmic...
Progesterone-mediated oocyte...
Metabolic pathways
Cell cycle - yeast
Pathways in cancer
MAPK signaling pathway
Hippo signaling pathway
Lysine degradation
Adherens junction
Renal cell carcinoma
Chronic myeloid leukemia
TGF-beta signaling pathway
Meiosis - yeast
Herpes simplex infection
Basal transcription factors
Dopaminergic synapse

◀**Fig. 6** Comparison of transcriptome expression profiles between normal, control and Ifrg15-specific siRNA-treated groups. **a** No DEGs were detected between the normal and negative control groups, but 1445 DEGs were generated between the groups treated with specific siRNAs against Ifrg15 and the two control groups. **b** Molecular function, biological processes of DEGs are shown in GO function annotation. **c** 1445 DEGs are shown after KEGG pathway analysis

damage is always followed by phosphorylation of the histone, H2AX, by the expression of kinases such as ATM, and γ-H2AX is the first step in recruiting and localizing DNA repair proteins [14]. Thus, we tested for the expressions of γ-H2AX and ATM. Unsurprisingly, much higher expression levels of γ-H2AX and ATM were observed in groups treated with the two Ifrg15-specific siRNA fragments. These results suggest that DNA damage might be one reason for the 1-cell blockage and the failure of male and female pronuclear fusion in mouse zygotes treated with specific siRNAs against Ifrg15.

Transcriptome sequencing using RNA-Seq technology is a powerful tool to obtain information within a short time and with enormous depth and coverage, and can broaden our knowledge of gene expression profiles in the preimplantation embryo [15]. We used untreated zygotes, and zygotes treated with non-silencing or specific siRNAs against Ifrg15, to carry out transcriptome sequencing analysis, GO enrichment analysis and functional annotation, as well as the prediction and identification of candidate genes. Thus we elucidated the regulatory mechanisms, and causes of failed cell cycle progress during embryo development, of mouse zygotes caused by Ifrg15-specific siRNAs.

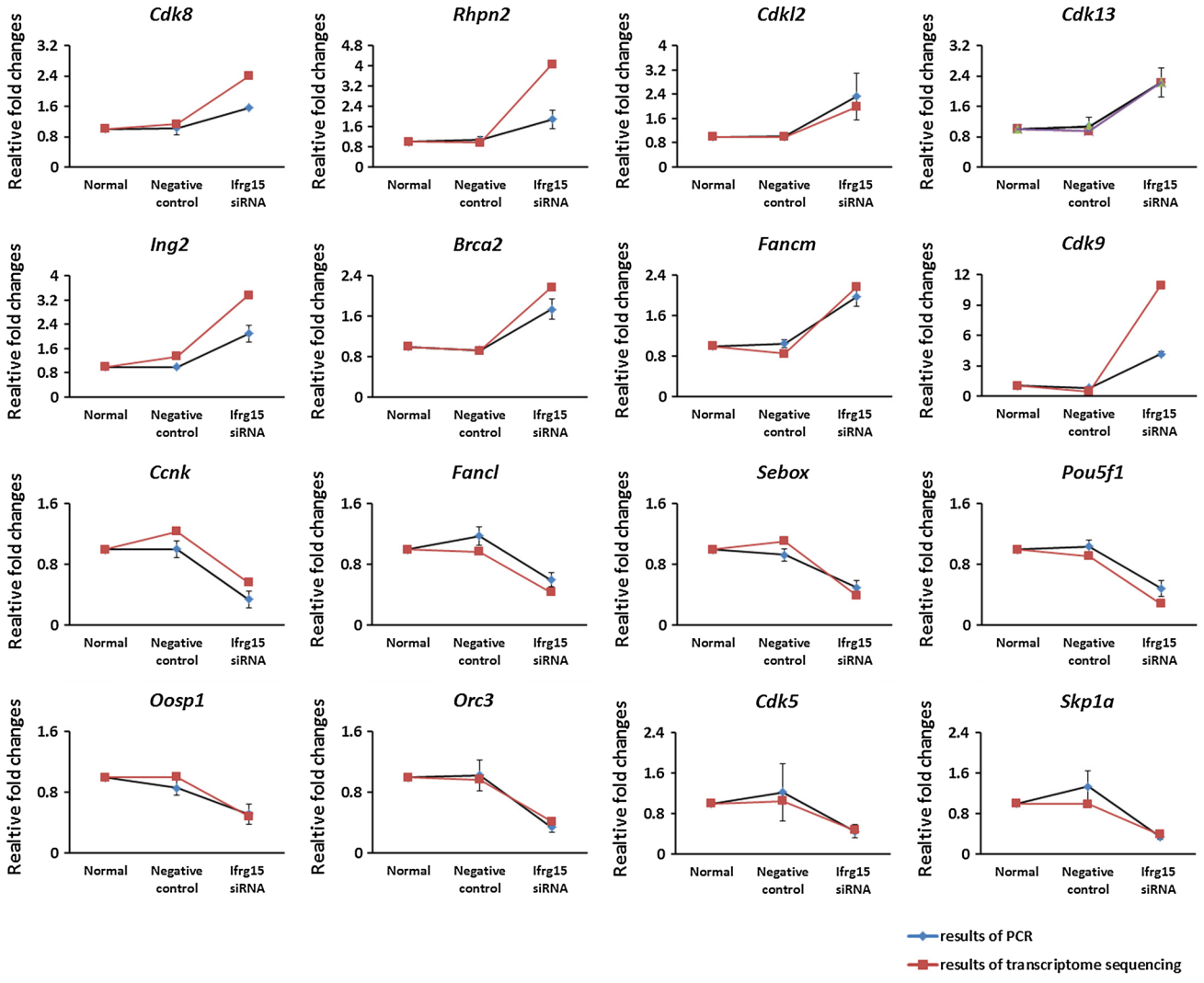

Fig. 7 Representative genes that were selected from upregulated and downregulated DEGs for subsequent qRT-PCR experiments. Cdk8, Rhpn2, Cdkl2, Cdk13, Ing2, Brca2, Fancm, and Cdk9 were upregulated, and Ccnk, Fancl, Sebox, Oct4, Oosp1, Orc3, Orc5, and Cdk5 were downregulated

We considered that more focus should be put on the delineation of DNA damage-related pathways and interactions in this model, not just on single molecular events. Indeed, in line with our observations of 197 genes enriched in 'biological process' GO terms based on 1445 DEGs, 12 pathways mainly involved in four aspects of 'DNA damage' (77 DEGs), 'DNA repair' (65 DEGs), 'cell cycle' (143 DEGs) and 'developmental process' (201 DEGs) were closely associated with DNA damage. Furthermore, about 1/3 of the 1445 DEGs were involved in these pathways. We propose that a cascade of gene activation or inactivation must be involved. In addition, database (http://biogps.org/#goto=welcome analysis) showed that many genes are almost only expressed in the mouse oocyte and zygotes such as Brca2, Gspt2, Oog4, Oosp1, Orc5 and Pdhx, which indicates that these genes play important roles during preimplantation development. For example, cyclin K and Fancl are important molecules involved in DNA damage, and several genes participate in the DNA damage response and genomic stability, such as RAD9, PARP1, BRCA1, and ATM. Orc3 and Orc5 are involved in DNA replication, and Oog4 and Pou5f1 are expressed in early mouse embryos or oocytes. Changes in the expression of the Ifrg15 gene could be associated with degradation of transcripts at the 1-cell stage, whereas other genes might undergo increased or decreased expression. Here we selected 55 representative DEGs to verify the accuracy of our qRT-PCR, and found that the expression trends of these genes were consistent with their transcriptomic expression profiles. We conclude that these DNA damage-related DEGs are direct or indirect target genes of Ifrg15, which play vital roles in maintaining DNA integrity and protecting DNA from damage.

Our study was slightly different from the report of Wu et al., who used qRT-PCR. They showed that mouse Ifrg15 mRNA was expressed in MII stage oocytes and preimplantation embryos, and peaked in blastocysts. They showed that Ifrg15 directly regulated the transcriptional levels of several key development-related genes such as Oct4, c-Myc and Nanog in a COS-7 cell line [9]. However, in the present study, we directly silenced Ifrg15 by microinjecting siRNA fragments against Ifrg15 into zygotes. We believed that this difference could be explained by the different research methods and cells used. In addition, 1-cell stage arrest or the failure of male and female pronuclear fusion is complex processes involving gene regulatory networks. Therefore, the large number of genes identified as involved in each phase is a first step toward analysis of these complex gene regulatory networks. Our results show that a single molecular change sometimes cannot provide the whole truth, so global profiling is essential to construct a molecular regulation blueprint and help us in understanding the molecular mechanism of preimplantation embryonic development.

In summary, we have uncovered many genes that have not been linked to DNA damage previously by determining the effect of IFRG15 depletion on mouse preimplantation embryo development. This protein might act to upregulate a cascade of genes involved in maintaining genomic stability and in allowing early mammalian embryogenesis to progress normally. The mechanisms and significance of early pronuclear fusion events, and how paternal and maternal genomes become enclosed within a single nuclear envelope might be interesting topics for future research. These results might have important implications for understanding human preimplantation embryo development.

Acknowledgments The authors thank all the members of the team for giving technical support and valuable suggestions. We gratefully acknowledge Liwen Bianji for editing the article. This research was supported by NSFC (Grant Nos.: 81270701, 81401204, 81471457).

References

1. Cedars M (2005) Introduction to infertility. In: Cedars M (ed) Infertility. McGraw-Hill, New York
2. Plachot M (2000) Fertilization. Hum Reprod 15(Suppl 4):19–30
3. Wright G et al (1990) Observations on the morphology of pronuclei and nucleoli in human zygotes and implications for cryopreservation. Hum Reprod 5(1):109–115
4. Johnson M (2007) Essential reproduction, 6th edn. Blackwell, Oxford
5. Wilson EB (1925) The cell in development and heredity. Macmillan, New York
6. Mayer W et al (2000) Spatial separation of parental genomes in preimplantation mouse embryos. J Cell Biol 148(4):629–634
7. Wang S et al (2010) Proteome of mouse oocytes at different developmental stages. Proc Natl Acad Sci USA 107(41):17639–17644
8. Yamaza H et al (2001) Detection of differentially expressed genes in the early developmental stage of the mouse mandible. Int J Dev Biol 45(4):675–680
9. Wu FR et al (2012) Sequence analysis, expression patterns and transcriptional regulation of mouse Ifrg15 during preimplantation embryonic development. Gene 507(2):119–124
10. Qi B et al (2007) Cloning and analysis of IFRG (interferon responsive gene) in rabbit oocytes and preimplantation embryos. Biocell 31(2):199–203
11. Zeng F, Schultz RM (2005) RNA transcript profiling during zygotic gene activation in the preimplantation mouse embryo. Dev Biol 283(1):40–57
12. Kigami D et al (2003) MuERV-L is one of the earliest transcribed genes in mouse one-cell embryos. Biol Reprod 68(2):651–654
13. Li L, Zheng P, Dean J (2010) Maternal control of early mouse development. Development 137(6):859–870
14. Kuo LJ, Yang LX (2008) Gamma-H2AX—a novel biomarker for DNA double-strand breaks. Vivo 22(3):305–309
15. Xiao M et al (2013) Transcriptome analysis based on next-generation sequencing of non-model plants producing specialized metabolites of biotechnological interest. J Biotechnol 166(3):122–134
16. Schefe JH et al (2006) Quantitative real-time RT-PCR data analysis: current concepts and the novel "gene expression's CT difference" formula. J Mol Med (Berl) 84(11):901–910